Research Square

Preprints are preliminary reports that have not undergone peer review.
They should not be considered conclusive, used to inform clinical practice,
or referenced by the media as validated information.

Osteotomy obliquity, contact area and working length in ulnar shortening osteotomy: a finite element analysis with a fixed implant

Zafer Gunes

zafergne@hotmail.com

Ankara Training and Research Hospital

Research Article

Keywords: Ulnar shortening osteotomy, Finite element analysis, Interfragmentary motion, Osteotomy obliquity, Working length, Contact area, Nonunion

Posted Date: October 29th, 2026

DOI: https://doi.org/10.21203/rs.3.rs-10722576/v1

License: This work is licensed under a Creative Commons Attribution 4.0 International License.
Read Full License

Additional Declarations: No competing interests reported.

Abstract

Background

Oblique ulnar shortening osteotomy (USO) is widely preferred over a transverse cut, and its clinical performance has been attributed to a larger contact surface at the osteotomy. In every published comparison, however, osteotomy geometry is confounded with the fixation system, and the proposed mechanism has not been tested biomechanically. Obliquity also lengthens the axial span of the cut, forcing the innermost screws apart and increasing screw working length.

Methods

A three-dimensional model of the distal ulna was built from a publicly available, anonymised CT-derived surface. A 3 mm shortening was simulated at obliquities of 40, 45, 60 and 90 degrees and fixed with an identical generic six-hole 3.5 mm volar locking plate. In Arm 1 screw positions were identical across obliquities, holding working length at 24.0 mm; in Arm 2 the construct followed clinical practice, with working length varying from 20.0 to 34.5 mm. Each configuration was loaded in axial compression (100 N), flexion and extension bending and torsion (1 N·m). All obliquities were additionally analysed with a 300 N interfragmentary lag screw preload under axial load and torsion, giving 40 nonlinear frictional-contact analyses in total.

Results

Without a lag screw, axial interfragmentary shear motion fell from 23.3 μm at 40 degrees to 21.6 μm at 45, 12.0 μm at 60 and 0.01 μm at 90 degrees, while the surface loaded in compression rose from 16% to 70%; despite the larger geometric area of an oblique cut, the absolute loaded area was therefore smaller. Torsion reversed this ordering, the 45 degree construct permitting 34% less shear motion than the transverse construct. At matched obliquity, the clinically scaled construct increased axial shear motion by 80% at 40 degrees and 48% at 45 degrees, and at angles of 45 degrees or less only two distal screws could be accommodated in the distal fragment. Addition of the lag screw preload reduced axial shear motion by 90 to 95% in the oblique constructs and raised the loaded contact area at 45 degrees to 87%, exceeding the transverse construct (80%).

Conclusions

The mechanical behaviour of an oblique ulnar shortening osteotomy depended strongly on whether interfragmentary compression was present. Without a lag screw the oblique construct permitted substantially greater interfragmentary shear under axial load and engaged less than a third as much loaded contact area than a transverse cut; with a lag screw the disadvantage was largely abolished and

the loaded contact area exceeded that of the transverse construct. The advantage of obliquity therefore appears to derive largely from the compression its geometry permits rather than from the geometry itself. Obliquity additionally imposes a longer working length and, at angles of 45 degrees or less, limits the distal fragment to two screws. Where reliable interfragmentary compression cannot be achieved, an oblique osteotomy cannot be assumed to retain the mechanical advantages usually attributed to it; where it can, the oblique configuration retains a torsional advantage that a transverse cut does not possess.

Background

Ulnar shortening osteotomy (USO) is among the most frequently performed procedures for ulnar impaction syndrome and for symptomatic positive ulnar variance after distal radius malunion[1, 2]. Delayed union and nonunion remain its principal complications. A systematic review of 37 studies comprising 1 423 patients placed the pooled nonunion rate at 4.0% and the pooled delayed union rate at 5.7%, although individual series have reported figures ranging from zero to almost one in five[3, 4].

The obliquity of the osteotomy has long been regarded as a determinant of healing. In the original description of the oblique technique, a 45 degree cut secured with an interfragmentary lag screw achieved union at a mean of 11 weeks against 21 weeks for transverse osteotomies in the same institution, and cadaveric testing showed significantly greater torsional rigidity for the oblique construct with no difference in anteroposterior or lateral bending[5]. That work established the 45 degree angle, which has been carried forward largely unchanged for three decades[6–9]. A widely used commercial osteotomy system nonetheless provides 40 degree reference marks rather than 45, and neither value derives from a biomechanical optimisation study.

Clinical comparisons of the two techniques have since accumulated, with mixed conclusions. The systematic review cited above found no significant difference in nonunion between transverse (4.16%) and oblique (3.86%) cuts, although delayed union was numerically less frequent after oblique osteotomy (4.1% versus 7.41%)[3]. A retrospective cohort of 92 patients reported a significant effect of oblique osteotomy on union rate and attributed this to the larger contact surface at the osteotomy site[10]. Comparative series have likewise reported shorter radiological healing times and lower implant removal rates after oblique osteotomy[11, 12]. Two features of this literature limit its interpretation. First, osteotomy geometry is systematically confounded with the implant: oblique osteotomies are generally performed with procedure-specific compression systems and locking screws, whereas transverse osteotomies are more often fixed with generic dynamic compression plates, so an apparent advantage of the cut may in fact reflect the fixation. Second, the mechanism most often invoked, namely a larger contact surface, refers to the geometric area of the cut and has never been tested against the area actually loaded in compression under physiological force.

A further and less appreciated consequence of obliquity is geometric. Because the cut traverses a bone of finite diameter, the axial extent of the osteotomy grows as the cut becomes more oblique. For a

diaphyseal diameter of approximately 12 mm, a transverse cut occupies no axial length, a 45 degree cut spans 12.2 mm and a 30 degree cut spans 21.1 mm. Screws must be placed clear of this zone, so surgeons lengthen the plate to preserve the number of screws on each fragment. This increases the distance between the innermost screws, that is, the screw working length, which is a principal determinant of interfragmentary movement in plate osteosynthesis[13, 14]. Obliquity and working length are therefore confounded in clinical practice as well.

Biomechanical data on this question remain sparse. Beyond the original cadaveric series, which tested torsion and bending but not axial compression, we are aware of only one finite element study of USO fixation, which compared volar with dorsal plate placement and found the volar position to produce lower interfragmentary strain[15]. Finite element analysis has been applied to fixation of the distal ulna in other contexts, comparing plate side and the number of distal screws in ulnar head fracture[16] and screw configuration in comminuted proximal ulnar fracture[17], but not to the obliquity of a shortening osteotomy. Computational work on USO itself has otherwise concentrated on distal radioulnar joint mechanics rather than on fixation stability[18, 19]. Osteotomy obliquity itself has not been examined computationally, and no study has separated the mechanical effect of the cut from that of the working length it imposes.

Finite element analysis is well suited to this problem because a single variable can be altered while every other feature of the construct is held constant, which is not achievable clinically. We therefore constructed a model of the distal ulna to address three questions. What is the effect of osteotomy obliquity on interfragmentary motion when the fixation construct is held identical? Does an oblique cut in fact increase the area of the osteotomy that is loaded in compression, as has been proposed? And how much of any effect of obliquity is attributable to the longer working length that clinical practice imposes?

Methods

Bone geometry

The construct and the study design are summarised in Fig. 1. A surface model of an adult right ulna was obtained from the NIH 3D Print Exchange (entry 3DPX-016810), a publicly available repository, under a Creative Commons Attribution 4.0 licence. No human participants or identifiable data were involved and institutional review board approval was therefore not required. Detailed donor demographics were not available from the repository.

The imported surface was regenerated on a 0.30 mm signed-distance grid and smoothed with a volume-preserving Taubin filter; the resulting volume differed from the input by 0.03%. Overall bone length was 284.7 mm. The distal 105 mm were retained for analysis, placing the fixed boundary more than 55 mm from the region of interest. At the osteotomy level the outer diameter was 12.2 mm, the medullary canal diameter 6.5 mm and the cortical area fraction 72%, all within published morphometric ranges for the ulnar diaphysis.

Cortical bone was defined as a uniform 3.0 mm shell obtained by Euclidean distance transform; the enclosed volume was assigned trabecular properties. Anatomical orientation was established from two landmarks: the interosseous crest, identified as the locus of maximum radial protrusion along the diaphysis, defined the lateral direction, and the ulnar styloid, identified as the most prominent feature within the distal 15 mm, resolved the volar-dorsal ambiguity. The assignment was verified by a fellowship-trained hand surgeon.

Implant model

A generic six-hole low-profile locking compression plate representative of commercially available ulnar shortening systems was modelled: 10 mm wide, 2.8 mm thick, with a bone-contacting surface conforming to the ulnar cortex at a uniform 0.10 mm offset. Dimensions were taken from published AO specifications for 3.5 mm implants[14]. A generic rather than a proprietary geometry was chosen so that the findings would not be specific to a single manufacturer.

Screws were modelled as 3.5 mm diameter cylinders traversing both cortices. Rather than introducing separate screw bodies with tied contact interfaces, which we found to produce spurious constraint-induced element distortion, screw regions were represented by assigning titanium properties to elements whose centroids lay within the screw envelope. This yields a fully bonded screw-bone interface, equivalent in effect to a tie constraint, without the numerical penalties of independently meshed cylindrical surfaces. Plate-to-bone load transfer through each screw was enforced by explicitly formulated multi-point constraints coupling the plate surface to the underlying cortical surface over the screw footprint, using quadratic triangular shape functions.

Material properties and contact

All materials were modelled as linear elastic and isotropic: cortical bone E = 17 000 MPa, trabecular bone E = 700 MPa, Ti-6Al-4V E = 110 000 MPa, all with Poisson's ratio 0.30.

Frictional contact with a coefficient of 0.30 was defined at the osteotomy interface and at the plate-bone interface, using a surface-to-surface penalty formulation permitting separation. The osteotomy surfaces were generated by cutting the regenerated bone surface with an analytical plane, which produced coincident planar faces with a mean initial separation of 0.018 mm.

Study design

Shortening was fixed at 3.0 mm along the bone axis for all models, deliberately below the 5 mm threshold above which distal radioulnar joint contact stress has been reported to rise[19, 20], so that joint loading would not confound the comparison. The osteotomy was placed 40 mm proximal to the distal articular surface, corresponding to the mid-point of the 3–5 cm range recommended by implant manufacturers.

Four obliquities were studied, defined as the angle between the osteotomy plane and the long axis of the bone: 40°, 45°, 60° and 90°, the last being a transverse cut. Two arms were analysed. In Arm 1, screw positions were identical in every model (10, 20 and 28 mm distally; 52, 60 and 70 mm proximally), giving a constant working length of 24.0 mm. In Arm 2, the construct followed clinical practice: the innermost screw on each fragment was placed 10 mm clear of the nearest cut edge, three screws were retained per fragment where anatomically possible, and the plate was lengthened accordingly. This yielded working lengths of 20.0, 27.0, 32.2 and 34.5 mm at 90°, 60°, 45° and 40° respectively. At 45° and 40°, only two distal screws could be accommodated between the osteotomy and the ulnar head. The four osteotomy configurations and their axial spans are shown in Fig. 1E.

A 30° configuration was attempted but could not be meshed reliably, because the cut intersects the cortical surface at so acute an angle that a slender wedge is produced at the fragment tip. This geometric difficulty parallels the clinical constraint: at 30° the axial span reaches 21.1 mm and no more than two distal screws can be placed.

The proximal cut surface was fully constrained. Four load cases were applied to the distal fragment: axial compression of 100 N distributed over the distal 12 mm, a magnitude consistent with the share of forearm axial load transmitted through the distal ulna[21], flexion and extension bending moments of 1 N·m, and a torsional moment of 1 N·m. Eight configurations and four load cases gave 32 analyses. Table 1 *summarises the model parameters.*

Table 1
Model parameters

Parameter	Value
Bone source	NIH 3D Print Exchange 3DPX-016810 (CC BY 4.0)
Total ulnar length	284.7 mm
Modelled segment	distal 105 mm
Diaphyseal outer diameter at osteotomy	12.2 mm
Medullary canal diameter	6.5 mm
Cortical area fraction	72%
Cortical thickness	3.0 mm (uniform)
Cortical bone	E = 17 000 MPa, v = 0.30
Trabecular bone	E = 700 MPa, v = 0.30
Implant (Ti-6Al-4V)	E = 110 000 MPa, v = 0.30
Plate	6-hole, 10 x 2.8 mm, volar, 0.10 mm offset
Screws	3.5 mm diameter, bicortical
Shortening	3.0 mm axial
Osteotomy level	40 mm proximal to distal articular surface
Obliquity (beta)	40, 45, 60, 90 degrees
Friction coefficient	0.30 (osteotomy and plate-bone)
Element type	C3D10 quadratic tetrahedra
Elements (reported analyses)	36 368
Solver	CalculiX 2.23

Discretisation and solution

Bodies were discretised with quadratic tetrahedral elements (C3D10) using a graded size field (Fig. 1D), refined to 0.75–1.15 mm within 13 mm of the osteotomy and around each screw, and coarsened to 3.4–4.6 mm remote from the region of interest. Mid-side nodes were retained at edge mid-points to avoid element inversion on curved boundaries.

Mesh convergence was assessed over four refinement levels of 15 530, 23 586, 36 368 and 54 042 elements for the 45° axial case. Between the two finest meshes, the 99th-percentile plate von Mises stress changed by 2.0%, the 99th-percentile cortical stress by 3.8% and interfragmentary shear motion by 5.0%. Peak nodal von Mises stress did not converge, increasing monotonically with refinement, which

is characteristic of a singularity at constraint boundaries; the 99th percentile was therefore adopted as the representative stress measure throughout. The 36 368-element discretisation was used for all reported analyses.

Analyses were solved with CalculiX 2.23. Interfragmentary motion was computed by projecting each node of the distal cut face onto the proximal cut surface and interpolating displacement, then decomposing the relative displacement into components normal and tangential to the osteotomy plane.

Results

Complete results for all configurations and load cases are given in Table 2. All analyses converged without element distortion or constraint failure. Newton-Raphson convergence was achieved within 17 iterations in the most demanding case.

Table 2
Complete results

Arm	β (°)	Distal screws	WL (mm)	Loading	IFM normal (µm)	IFM shear (µm)	Contact (%)	Plate σvM p99 (MPa)	Cortical σvM p99 (MPa)
1	40	3	24.0	Axial	6.8	23.3	16	28.3	7.0
				Flexion	6.4	6.6	11	25.2	10.2
				Extension	3.4	7.6	8	22.0	9.5
				Torsion	19.4	32.9	3	36.8	26.4
1	45	3	24.0	Axial	4.5	21.6	22	25.3	6.5
				Flexion	6.8	5.5	6	25.1	11.1
				Extension	3.3	6.7	9	21.2	10.6
				Torsion	19.0	39.4	3	38.4	29.3
1	60	3	24.0	Axial	1.2	12.0	29	18.9	7.7
				Flexion	6.8	3.7	4	25.9	12.3
				Extension	3.0	4.8	10	21.3	11.8
				Torsion	12.9	42.5	7	41.3	34.2
1	90	3	24.0	Axial	0.0	0.0	70	3.2	2.8
				Flexion	9.4	2.3	4	27.2	12.5
				Extension	2.8	0.5	15	17.5	10.3
				Torsion	0.0	59.4	48	51.4	40.5
2	40	2	34.5	Axial	15.3	42.0	10	37.3	13.9
				Flexion	10.6	10.9	11	31.9	14.2
				Extension	7.4	16.3	6	29.7	13.7
				Torsion	32.2	51.1	2	42.3	32.9
2	45	2	32.2	Axial	7.9	32.0	13	40.3	16.3
				Flexion	10.2	11.8	3	38.7	18.0
				Extension	3.9	16.5	9	38.1	17.6
				Torsion	21.0	43.5	2	53.6	32.3
2	60	3	27.0	Axial	1.6	14.6	25	23.7	13.6

Arm	β (°)	Distal screws	WL (mm)	Loading	IFM normal (µm)	IFM shear (µm)	Contact (%)	Plate σvM p99 (MPa)	Cortical σvM p99 (MPa)
				Flexion	10.9	3.2	3	31.3	14.5
				Extension	3.0	6.6	12	27.7	15.5
				Torsion	11.9	39.0	7	43.2	34.3
2	90	3	20.0	Axial	0.0	0.0	74	3.1	2.6
				Flexion	8.2	1.6	4	27.5	11.3
				Extension	2.1	0.4	15	17.1	9.2
				Torsion	0.9	37.4	0	39.4	28.7
1 + lag	40	3	24.0	Axial	0.1	1.6	78	6.6	8.6
1 + lag		3		Torsion	0.5	6.6	39	21.1	16.0
1 + lag	45	3	24.0	Axial	0.1	1.1	87	8.8	9.4
1 + lag		3		Torsion	0.6	7.5	42	21.6	18.2
1 + lag	60	3	24.0	Axial	0.2	1.2	72	17.8	7.4
1 + lag		3		Torsion	1.6	11.1	35	27.1	22.9
1 + lag	90	3	24.0	Axial	0.1	0.1	80	4.9	4.4
1 + lag		3		Torsion	0.1	16.0	71	27.1	26.8

Arm 1 + lag denotes the fixed construct with a 300 N interfragmentary lag screw preload. Values < 0.05 µm are reported to two decimal places

Effect of obliquity at constant working length (Arm 1)

Under axial compression, interfragmentary shear motion decreased monotonically as the osteotomy approached the transverse plane (Fig. 2A). Mean shear motion was 23.3 µm at 40°, 21.6 µm at 45°, 12.0 µm at 60° and 0.01 µm at 90°. The proportion of the osteotomy surface in compressive contact rose in parallel (Fig. 2B), from 16% at 40° to 22% at 45%, 29% at 60% and 70% at 90°. The 99th-percentile plate von Mises stress fell from 28.3 MPa to 3.2 MPa across the same range (Fig. 2D), indicating a

progressive transfer of load from the implant to the bone as the interface became more nearly perpendicular to the applied force.

Bending followed the same ordering. In flexion, shear motion fell from 6.6 μm at 40° to 2.3 μm at 90°; in extension, from 7.6 μm to 0.5 μm.

Torsion reversed the pattern (Fig. 2A). Shear motion rose from 32.9 μm at 40° to 39.4 μm at 45°, 42.5 μm at 60° and 59.4 μm at 90°. The 45° construct therefore permitted 34% less interfragmentary shear than the transverse construct under torsional load. Plate stress in torsion increased correspondingly, from 36.8 MPa at 40° to 51.4 MPa at 90°.

Torsion produced the largest interfragmentary motion of any load case in every configuration, exceeding axial compression by a factor of 1.4 at 40° and by three orders of magnitude at 90°. The redistribution of stress that underlies this reversal is shown in Fig. 3: under axial load the oblique construct carries load through the plate, whereas the transverse construct carries it through bone, and under torsion the pattern is inverted.

Effect of working length (Arm 1 versus Arm 2)

Comparison of the two arms at matched obliquity isolated the effect of working length (Fig. 2C). Under axial compression, the clinically scaled construct increased interfragmentary shear motion by 80% at 40° (23.3 to 42.0 μm), by 48% at 45° (21.6 to 32.0 μm) and by 21% at 60° (12.0 to 14.6 μm). The transverse construct was essentially unaffected, its working length being shorter in the clinical arm than in the fixed arm (20.0 versus 24.0 mm).

Plate stress increased in parallel: at 45°, the 99th-percentile plate von Mises stress rose from 25.3 MPa in the fixed construct to 40.3 MPa in the clinical construct under axial load.

The magnitude of the working-length penalty therefore scaled with obliquity, because obliquity determines how far apart the innermost screws must be placed.

Effect of interfragmentary lag screw compression

Addition of a 300 N interfragmentary lag screw preload transformed the behaviour of the oblique constructs under axial load (Fig. 4). Interfragmentary shear motion fell from 23.3 to 1.6 μm at 40 degrees (a 93% reduction), from 21.6 to 1.1 μm at 45 degrees (95%) and from 12.0 to 1.2 μm at 60 degrees (90%). The proportion of the osteotomy surface loaded in compression rose from 16% to 78% at 40 degrees, from 22% to 87% at 45 degrees and from 29% to 72% at 60 degrees. At 45 degrees the loaded contact area with a lag screw (87%) exceeded that of the transverse construct (80%) (Fig. 4B). The 99th-percentile plate von Mises stress fell correspondingly, from 25.3 to 8.8 MPa at 45 degrees, indicating that load was again being carried by bone rather than by the implant.

Under torsion the ordering between obliquities was preserved (Fig. 4C), the oblique constructs remaining superior, but all values fell by roughly three quarters: from 39.4 to 7.5 μm at 45 degrees and from 59.4 to 16.0 μm at 90 degrees.

The transverse construct, to which a lag screw is not conventionally applied, also benefited: loaded contact area rose from 70% to 80% and torsional shear motion fell from 59.4 to 16.0 μm.

Interfragmentary strain

As a supportive analysis, and assuming a nominal interfragmentary gap of 0.5 mm rather than a model-derived gap, shear strain at the osteotomy in the fixed construct was 4.7% at 40°, 4.3% at 45%, 2.4% at 60% and 0.002% at 90° under axial load, and 6.6%, 7.9%, 8.5% and 11.9% respectively under torsion. Varying the assumed gap between 0.25 and 1.0 mm scaled these values proportionally but did not alter the ordering between configurations. Under torsion with a 0.25 mm gap, shear strain in the 45° construct reached 15.8%, exceeding the upper bound of the interfragmentary strain window generally regarded as favourable for secondary bone healing.

Discussion

This study set out to separate three variables that are confounded in clinical practice: the geometry of the osteotomy, the screw working length that geometry imposes, and the interfragmentary compression that geometry permits. Three findings emerged. The mechanical behaviour of an oblique cut under axial load is markedly worse than that of a transverse cut when no compression is applied; this disadvantage is largely abolished by a lag screw preload; and, independently of both, the longer working length that an oblique cut requires in clinical constructs increases interfragmentary shear by a further half to four fifths.

The mechanism underlying the first finding is straightforward. An axial force applied across a transverse interface resolves almost entirely into a normal compressive component, which the bone carries directly. As the interface becomes oblique, an increasing fraction of that force resolves into a shear component that an uncompressed interface cannot resist, so the fragments slide and the load path is diverted through the plate. The progressive fall in plate stress from 28.3 MPa at 40 degrees to 3.2 MPa at 90 degrees under axial load is a direct expression of this transfer, and the redistribution is evident in the stress fields of Fig. 3.

This distinction matters because normal and shear interfragmentary motion are not biologically equivalent. Moderate axial micromotion is recognised as a stimulus to callus formation[20, 22], whereas shear motion of comparable magnitude has been associated with delayed union and with the formation of fibrous rather than osseous tissue at the interface[21, 23]. A configuration that converts axial load into interfragmentary shear is therefore unfavourable in a manner that a measurement of total motion alone would not reveal.

Our results also bear on the mechanism most often invoked to explain the clinical performance of the oblique cut. A larger contact surface has been proposed as the reason for improved union after oblique osteotomy[10]. The geometric area of an oblique cut is indeed larger, by a factor of 1.41 at 45 degrees. Under axial load without compression, however, only 22% of that surface was engaged in the present model, against 70% for the transverse cut, so the absolute loaded area was substantially smaller. The distinction between the geometric area of a cut and the area actually engaged under load appears not to have been drawn previously.

Adding a lag screw preload reversed this picture. Interfragmentary shear motion in the oblique constructs fell by 90 to 95%, and the loaded contact area at 45 degrees rose to 87%, exceeding the transverse construct. The larger contact surface proposed in the clinical literature is therefore real, but conditional: obliquity creates the potential for a larger loaded interface, and compression is what realises it. On this reading the biomechanical value of an oblique osteotomy derives less from the geometry of the cut than from the compression that geometry permits.

This offers an interpretation of the clinical literature. In the pooled analysis of 1 423 patients the difference in nonunion between oblique and transverse techniques was not statistically significant[3], and the evidence favouring the oblique cut rests mainly on delayed union and time to radiological healing. In essentially every published comparison, however, osteotomy geometry is confounded with the implant: oblique osteotomies are generally performed with procedure-specific systems providing controlled compression and locking fixation, whereas transverse osteotomies are more often fixed with generic dynamic compression plates[10–12, 24]. Comparative series have also reported lower rates of implant removal after oblique osteotomy[11, 25]. A recent comparison of an oblique locking compression system with a transverse non-locking system found faster union and less delayed union in the oblique group[12]; interpreted through the present results, that difference may be attributable at least in part to the compression achieved by the former system rather than to the angle of the cut alone.

The torsional results provide a point of comparison with earlier experimental work. Rayhack and colleagues reported significantly greater torsional rigidity for the oblique construct in cadaveric testing[5], and the present model reproduces this: the 45 degree construct permitted 34% less interfragmentary shear than the transverse construct under torsion, an ordering preserved with and without lag screw compression. The same cadaveric study reported no difference in anteroposterior or lateral bending, whereas the present analysis found an advantage for the transverse cut in both bending directions. The two measurements are not equivalent. Cadaveric testing quantifies the global stiffness of the construct, whereas the present analysis quantifies relative displacement at the interface; two constructs may possess similar overall stiffness while distributing deformation differently between implant and interface. This qualitative agreement in torsion supports the plausibility of the model but does not constitute experimental validation.

The second principal finding concerns working length. Because an oblique cut occupies a longer axial span, the innermost screws must be placed further apart, and a surgeon who preserves the number of

screws by lengthening the plate necessarily lengthens the working length. At matched obliquity, the clinically scaled construct increased axial interfragmentary shear by 48% at 45 degrees and by 80% at 40 degrees. This penalty is entailed by obliquity rather than incidental to it, and it acts in the same direction as the geometric effect. The sensitivity of interfragmentary motion to screw configuration that we observe is consistent with computational work on the proximal ulna, in which screw arrangement altered both interfragmentary motion and the distribution of stress within the plate[17]. It also implies that series reporting the osteotomy angle without reporting plate length and screw configuration are not directly comparable, which may contribute to the dispersion of published outcomes.

A third constraint emerged from the geometry itself. At obliquities of 45 degrees and below, no more than two screws could be placed in the distal fragment between the osteotomy and the ulnar head, because the usable diaphysis distal to the cut is only some 30 mm in length. Reduction from three to two distal screws has been shown in finite element analysis of distal ulnar fixation to alter both construct stress and stability[16], so the constraint is not merely nominal. At 30 degrees the axial span of the cut reaches 21.1 mm and the configuration could not be meshed reliably, the cut intersecting the cortex at so acute an angle that a slender wedge is produced at the fragment tip. This computational difficulty has a clinical counterpart: very oblique cuts leave progressively less bone for distal fixation, at precisely the fragment that is least well supported.

These observations have a specific intraoperative corollary. Compression may be lost at the moment it is applied: when the lag screw crosses the far cortex the cortex may crack or the thread may fail to purchase, and the compression generated is then partly or wholly lost. The osteotomy nevertheless remains radiographically apposed, and the natural inference at operation is that apposition is sufficient. The present results suggest that apposition and compression should not be treated as equivalent. With the fragments in contact but uncompressed, only 22% of the 45 degree osteotomy surface carried load under axial force and interfragmentary shear motion was roughly twenty times greater than in the compressed construct, whereas a transverse cut in the same situation retained 70% loaded contact area. The oblique configuration therefore appears the more vulnerable of the two to loss of compression. It should be noted that some procedure-specific plates generate compression through a dynamic compression slot independently of the lag screw, in which case compression may be preserved despite lag screw failure.

A secondary observation deserves mention. The transverse construct also benefited from the applied preload, its torsional interfragmentary shear falling from 59.4 to 16.0 μm and its loaded contact area rising from 70% to 80%. Interfragmentary compression beyond that provided by the plate itself is not conventionally sought in transverse USO, and whether a dedicated compression screw would improve outcomes in that setting has not been investigated clinically.

Taken together, these results do not indicate that oblique osteotomy should be abandoned. Forearm rotation generates torsional load, and the oblique configuration was superior in that mode under all conditions tested. Rather, obliquity and compression emerge as a single decision rather than two. Where

reliable interfragmentary compression can be achieved, an oblique osteotomy is biomechanically sound and retains a torsional advantage the transverse cut does not possess. Where compression cannot be achieved or is lost, an oblique cut cannot be assumed to retain the mechanical advantages usually attributed to it, and may be at a disadvantage relative to a transverse cut under axial load. A transverse or minimally oblique cut may therefore merit consideration where distal fixation is limited or where compression is uncertain.

Several limitations should be acknowledged. Most importantly, the model was not validated against experimental displacement or stiffness measurements; the agreement with published cadaveric torsional data is qualitative and directional rather than quantitative. The model is based on a single bone geometry, of unknown donor demographics, so the results may to some degree be geometry-specific; the analysis is comparative within a single model rather than predictive of absolute values, and every configuration shares the identical bone, implant, mesh and boundary conditions, so differences between configurations cannot be attributed to variation in the underlying bone morphology. Material properties were assigned as homogeneous linear elastic isotropic regions rather than mapped from Hounsfield units, and cortical anisotropy was not represented. The analysis is static and represents neither cyclic loading nor progressive healing; callus tissue was not modelled, so the results describe the immediate postoperative mechanical environment. Screws were represented by material assignment within the screw envelope rather than as threaded bodies, giving a fully bonded screw-bone interface; this corresponds to the immediate condition of a locking construct rather than to a loosening interface and may overestimate interface stiffness. The lag screw was represented by a preload rather than as an explicit structural component, so its contribution to construct stiffness after preload application was not captured, and a single preload magnitude of 300 N was used without a formal sensitivity analysis. Finally, interfragmentary strain was computed against an assumed nominal gap rather than a model-derived gap; these values are presented as a supportive analysis rather than as a primary outcome, and although the sensitivity analysis showed the ordering of configurations to be unaffected by the assumption, they should not be interpreted as predictions of healing.

Conclusions

In this finite element analysis with a fixed implant, the mechanical behaviour of an oblique ulnar shortening osteotomy depended strongly on whether interfragmentary compression was present. Without a lag screw, the oblique construct permitted substantially greater interfragmentary shear motion under axial load and engaged less than a third as much of the osteotomy surface in compression as a transverse cut; with a 300 N lag screw preload, shear motion fell by 90 to 95% and the loaded contact area at 45 degrees exceeded that of the transverse construct. The advantage of obliquity therefore appears to derive largely from the compression its geometry permits rather than from the geometry itself. Obliquity additionally imposes a longer screw working length, increasing axial interfragmentary shear by a further 48 to 80%, and at angles of 45 degrees or less limits the distal fragment to two screws. Where compression cannot be reliably achieved, an oblique osteotomy cannot be assumed to

retain the mechanical advantages usually attributed to it; where it can, the oblique configuration retains a torsional advantage that a transverse cut does not possess.

Declarations

Ethics approval and consent to participate

Not applicable. No human participants, human material or human data were involved. The geometric model was derived from a publicly available, fully anonymised surface model distributed under a Creative Commons Attribution 4.0 licence (NIH 3D Print Exchange, entry 3DPX-016810). Institutional review board approval was therefore not required.

Consent for publication

Not applicable.

Availability of data and materials

The bone surface model is publicly available from the NIH 3D Print Exchange (3DPX-016810). The complete computational pipeline, the source geometry, the model configuration files and solver-ready CalculiX input decks for all 40 analyses reported in this study are provided as Supplementary Material (Supplementary Data 1: source code, geometry and documentation; Supplementary Data 2: input decks), enabling independent inspection and reproduction of the finite element analyses.

Competing interests

The author declares no competing interests. No implant manufacturer provided funding, materials, or geometric data. The plate modelled was a generic design derived from published AO specifications and does not correspond to any proprietary product.

Funding

This research received no specific grant from any funding agency in the public, commercial or not-for-profit sectors.

Authors' contributions

ZG is the sole author. ZG conceived and designed the study, defined the clinical question and the surgically relevant construct configurations, developed and verified the finite element model set-up, verified the anatomical orientation of the model, assessed mesh convergence and boundary conditions, performed and interpreted the analyses, and drafted and critically revised the manuscript. The author read and approved the final manuscript and takes full responsibility for all aspects of the work.

Acknowledgements

The authors thank the contributor of entry 3DPX-016810 to the NIH 3D Print Exchange for making the bone surface model publicly available.

References

1. MILCH, H., *CUFF RESECTION OF THE ULNA FOR MALUNITED COLLES'FRACTURE.* JBJS, 1941. **23**(2): p. 311-313.
2. Chun, S. and A.K. Palmer, *The ulnar impaction syndrome: follow-up of ulnar shortening osteotomy.* J Hand Surg Am, 1993. **18**(1): p. 46-53.
3. Owens, J., et al., *Nonunion Rates Among Ulnar-Shortening Osteotomy for Ulnar Impaction Syndrome: A Systematic Review.* J Hand Surg Am, 2019. **44**(7): p. 612.e1-612.e12.
4. Zhang, Y., et al., *Risk Factors for Complications in Ulnar Shortening Osteotomies: A Multicenter Retrospective Review.* J Hand Surg Am, 2025. **50**(1): p. 104.e1-104.e7.
5. Rayhack, J.M., et al., *Precision oblique osteotomy for shortening of the ulna.* J Hand Surg Am, 1993. **18**(5): p. 908-18.
6. Labosky, D.A. and C.A. Waggy, *Oblique ulnar shortening osteotomy by a single saw cut.* J Hand Surg Am, 1996. **21**(1): p. 48-59.
7. Mizuseki, T., K. Tsuge, and Y. Ikuta, *Precise ulna-shortening osteotomy with a new device.* J Hand Surg Am, 2001. **26**(5): p. 931-9.
8. Chen, N.C. and S.W. Wolfe, *Ulna shortening osteotomy using a compression device.* J Hand Surg Am, 2003. **28**(1): p. 88-93.
9. Sunil, T.M., et al., *A comparative study of ulnar-shortening osteotomy by the freehand technique versus the Rayhack technique.* J Hand Surg Am, 2006. **31**(2): p. 252-7.
10. Kasper, A.A., et al., *Nonunion After Using Procedure-Specific Instrumentations for Ulnar Shortening Osteotomy.* Arch Bone Jt Surg, 2023. **11**(11): p. 677-683.
11. Singhal, R., et al., *A Study Comparing the Outcomes of Transverse Ulnar Shortening Osteotomy Fixed with a DCP to Oblique Osteotomy Fixed with a Procedure Specific Plate.* J Hand Surg Asian Pac Vol, 2020. **25**(4): p. 441-446.
12. Miyashima, Y., et al., *Comparison of dynamic compression plate systems with oblique osteotomy and locking plate fixation versus transverse osteotomy and non-locking plate fixation for ulnar shortening osteotomy.* J Orthop Sci, 2025. **30**(5): p. 798-804.
13. Stoffel, K., et al., *Biomechanical testing of the LCP--how can stability in locked internal fixators be controlled?* Injury, 2003. **34 Suppl 2**: p. B11-9.
14. Gautier, E. and C. Sommer, *Guidelines for the clinical application of the LCP.* Injury, 2003. **34 Suppl 2**: p. B63-76.
15. Zhang, C.L. and L.F. Dai, *Biomechanical evaluation of plate positioning in ulnar shortening osteotomy for nonunion prevention.* Proc Inst Mech Eng H, 2026. **240**(1): p. 25-33.

16. Zhang, Y., et al., *Finite element analysis of different locking plate fixation methods for the treatment of ulnar head fracture.* J Orthop Surg Res, 2021. **16**(1): p. 191.
17. Šafran, J., et al., *Analysing plate fixation of a comminuted fracture of the proximal ulna in relation to the elbow joint: a finite element study.* J Orthop Surg Res, 2025. **20**(1): p. 712.
18. Greybe, D., et al., *A finite element model to investigate the effect of ulnar variance on distal radioulnar joint mechanics.* Int J Numer Method Biomed Eng, 2017. **33**(2).
19. Tan, J., et al., *Effect of different ulnar osteotomies on loading of the distal radioulnar joint: a finite element analysis.* BMC Musculoskelet Disord, 2024. **25**(1): p. 454.
20. Nishiwaki, M., et al., *Ulnar-shortening effect on distal radioulnar joint pressure: a biomechanical study.* J Hand Surg Am, 2008. **33**(2): p. 198-205.
21. Shaaban, H., et al., *The distal radioulnar joint as a load-bearing mechanism--a biomechanical study.* J Hand Surg Am, 2004. **29**(1): p. 85-95.
22. Perren, S.M., *Physical and biological aspects of fracture healing with special reference to internal fixation.* Clin Orthop Relat Res, 1979(138): p. 175-96.
23. Augat, P., et al., *Shear movement at the fracture site delays healing in a diaphyseal fracture model.* J Orthop Res, 2003. **21**(6): p. 1011-7.
24. Claes, L.E., et al., *Effects of mechanical factors on the fracture healing process.* Clin Orthop Relat Res, 1998(355 Suppl): p. S132-47.
25. Pomerance, J., *Plate removal after ulnar-shortening osteotomy.* J Hand Surg Am, 2005. **30**(5): p. 949-53.

Figures

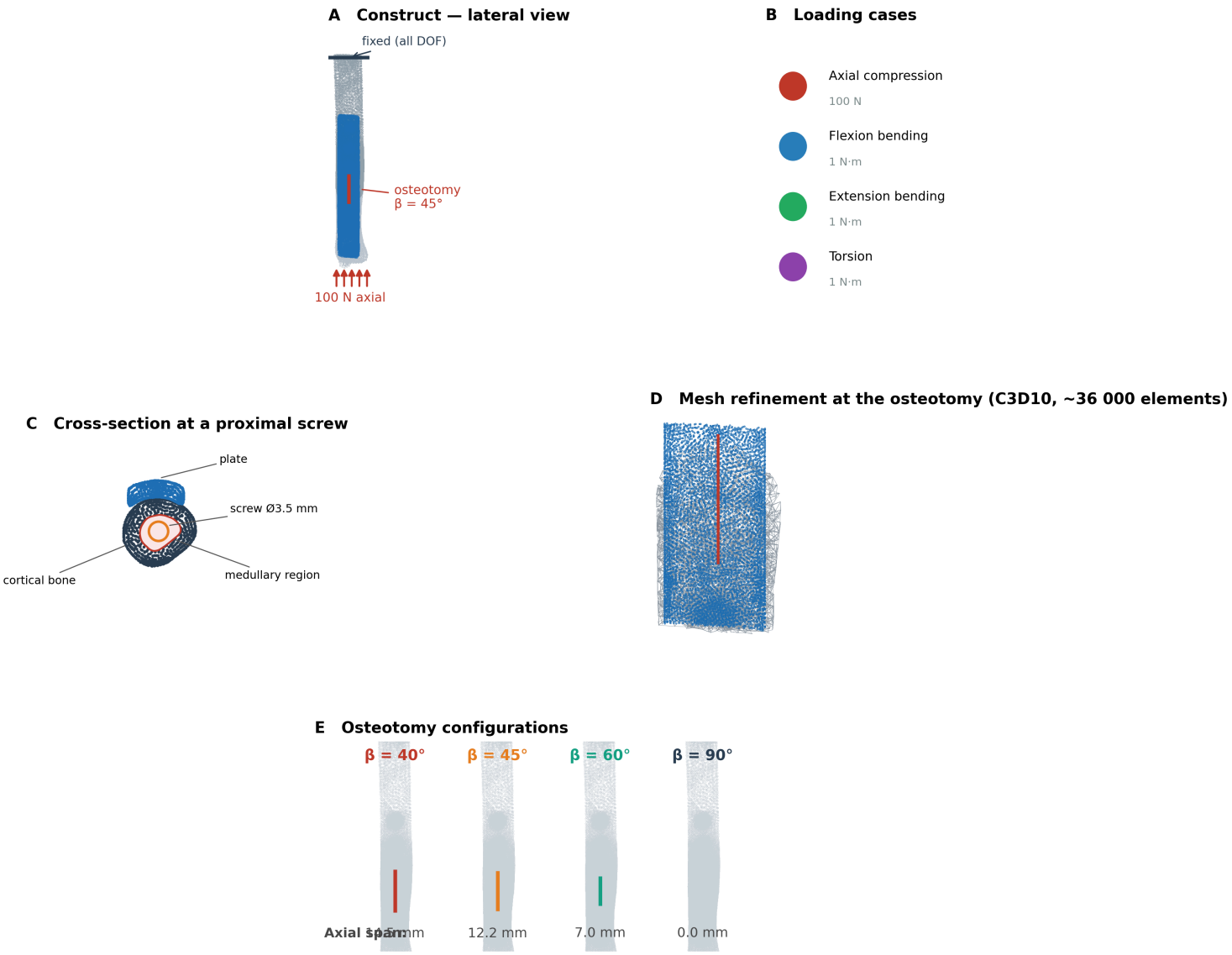


Figure 1

Model construction and study design. (A) The construct in lateral view, showing the distal 105 mm of the ulna, the volar six-hole plate, screw positions and the osteotomy plane; the proximal cut surface was fully constrained and axial load was applied to the distal fragment. (B) The four load cases. (C) Cross-section at a proximal screw showing cortical bone, medullary region, plate and the 3.5 mm screw envelope. (D) Graded mesh refinement around the osteotomy. (E) The four osteotomy configurations with their axial spans; the span of the cut increases from 0 mm at 90 degrees to 14.5 mm at 40 degrees.

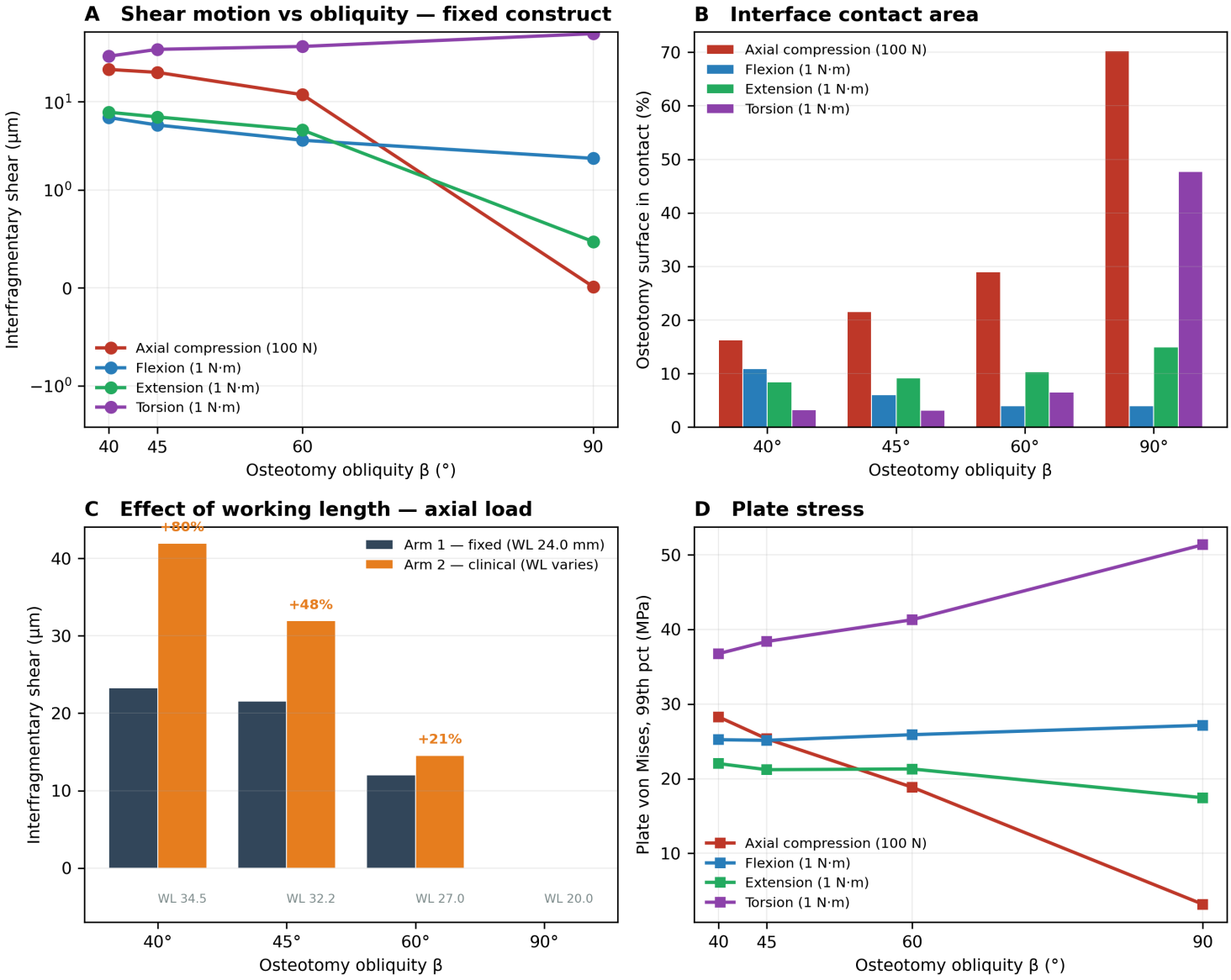


Figure 2

Effect of osteotomy obliquity with the fixation construct held constant (Arm 1). (A) Interfragmentary shear motion against obliquity for each load case; note the symmetrical logarithmic ordinate. (B) Proportion of the osteotomy surface loaded in compression. (C) Comparison of the fixed construct (Arm 1, working length 24.0 mm) with the clinically scaled construct (Arm 2) under axial load; percentages denote the increase attributable to the longer working length, which is annotated beneath each pair. (D) 99th-percentile plate von Mises stress.

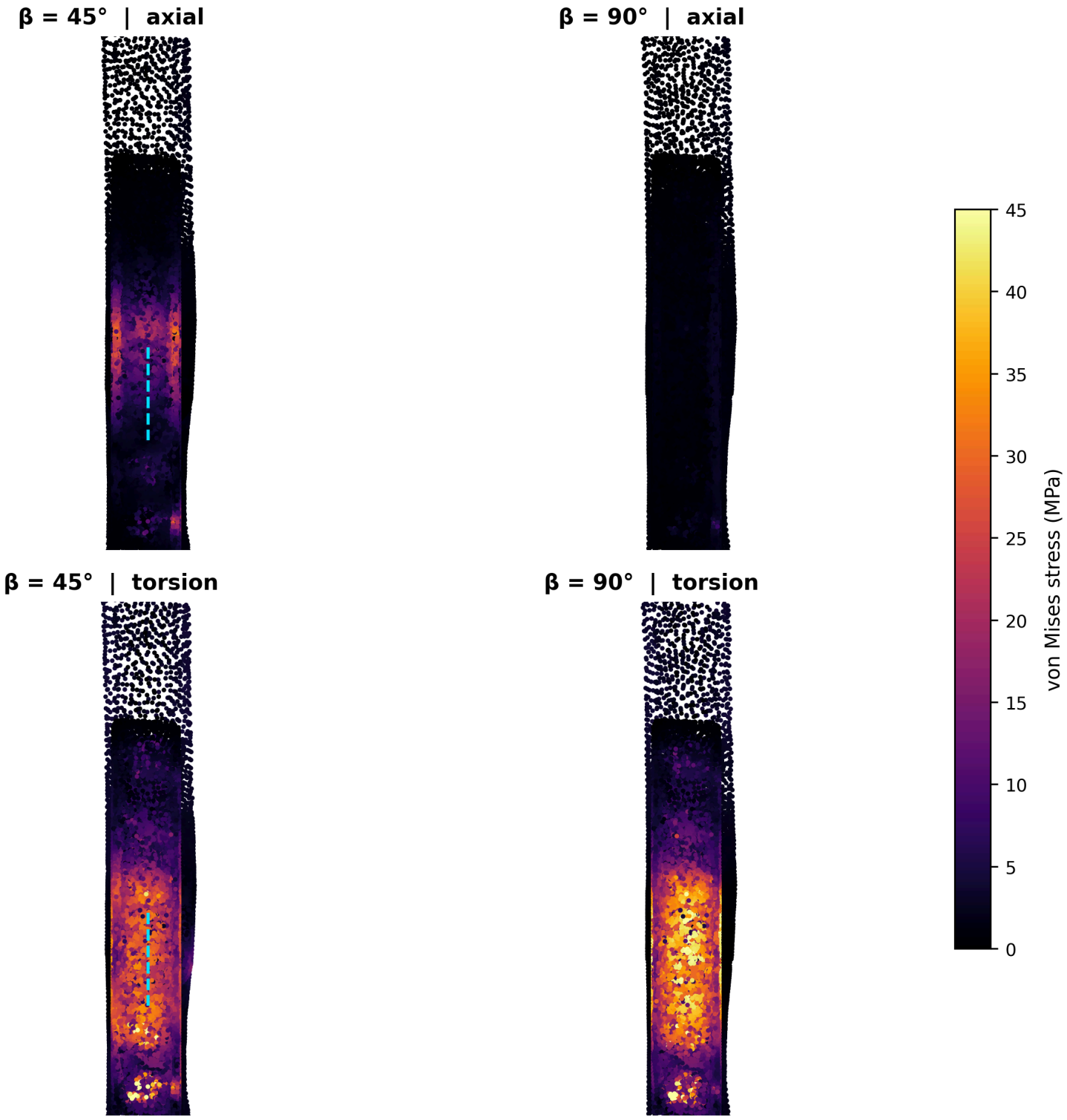


Figure 3

Von Mises stress distribution in the 45 degree and 90 degree constructs under axial compression and torsion. The dashed line marks the osteotomy plane. Under axial load the oblique construct transmits load through the plate, whereas the transverse construct transmits it through bone; under torsion the pattern is reversed.

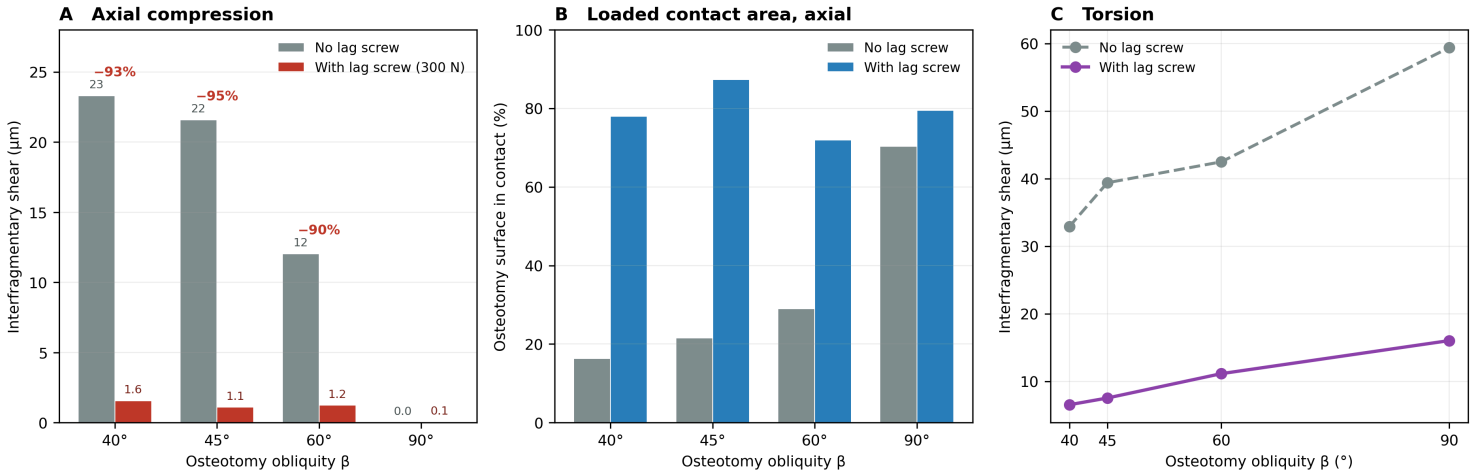


Figure 4

Effect of a 300 N interfragmentary lag screw preload. (A) Interfragmentary shear motion under axial compression with and without the lag screw; percentages denote the reduction. (B) Proportion of the osteotomy surface loaded in compression under axial load; with a lag screw the 45 degree construct exceeds the transverse construct. (C) Interfragmentary shear motion under torsion, where the ordering between obliquities is preserved.

Supplementary Files

This is a list of supplementary files associated with this preprint. Click to download.

- SupplementaryData1pipelinesourcecodegeometryconfigurationdocumentation.zip
- SupplementaryData240CalculiXinputdecks.zip